Available online at www.sciencedirect.com
SCIENCE DIRECT®
ELSEVIER
Journal of Hydrology 315 (2005) 203–219
Journal of Hydrology
www.elsevier.com/locate/jhydrol

Considerations for the use of radar-derived precipitation estimates in determining return intervals for extreme areal precipitation amounts

Robert J. Allen[a], Arthur T. DeGaetano[b,*]

[a]Department of Geology and Geophysics, Yale University, New Haven, CT, USA
[b]Northeast Regional Climate Center, Department of Earth and Atmospheric Science, 1119 Bradfield Hall, Cornell University, Ithaca, NY 14853, USA

Received 13 February 2004; revised 24 March 2005; accepted 31 March 2005

Abstract

To explore the feasibility of radar-based extreme precipitation climatologies, prototype radar areal reduction factor (ARF) curves are developed and compared to those based on traditional rain gauge networks. For both the radar and gauge data, increasing the spatial density of observations has little influence on the ARF relationship. However, independently, considerable differences between radar ARF and gauge ARF exist. Radar ARF decays at a faster rate (with increasing area) than gauge ARF. For a basin size of 20,000 km^2, the percent difference between radar ARF and gauge ARF ranges from 11 to 32%. This implies that radar-derived estimates of extreme point precipitation are disproportionately larger than radar-derived estimates of extreme areal precipitation, as compared to the corresponding relationship based on rain gauges.

Between-station variance of same-day extreme precipitation, as well as the coefficient of variation tends to be larger for the radar-derived areal extreme events, favoring a smaller radar areal precipitation. Smaller radar ARF is also favored because, on average, a higher percentage of gauges have coincident annual maxima than do the radar pixels that correspond to these gauges. Radar ARF curves computed based on gauge-calibrated radar data decay at an even faster rate than the unadjusted radar ARF. The accuracy of the calibrated radar data for these extreme events is suspect, however.

Areal precipitation amounts for the 2-, 5- and 10-year return period were computed by fitting an extreme value distribution to the areal radar, (and separately gauge), maxima from 5 years of available data. In one study area, the radar estimates tend to exceed those based on the gauge, whereas in a different region the gauge estimates tend to exceed those based on the radar. These results emphasize that a smaller radar ARF does not necessarily imply a lower radar mean areal precipitation.

Keywords: Radar rainfall; Areal reduction factors; Extreme value analysis; Raingauge; Rainfall estimates

1. Introduction

Contemporary US National Weather Service (NWS) radars are capable of providing precipitation

* Corresponding author.
E-mail address: atd2@cornell.edu (A.T. DeGaetano).

0022-1694/$ - see front matter
doi:10.1016/j.jhydrol.2005.03.028

estimates at spatial and temporal resolutions unmatched by conventional rain gauge networks. It is feasible these data could transform the procedures by which extreme areal precipitation return periods are currently computed, once an adequate historical record of radar-based precipitation observations becomes available. Each radar umbrella is essentially a dense measuring network with large areal coverage ($>50{,}000$ km^2), as well as high spatial (~ 2 km^2) and temporal (15–30 min) resolution.

Given the limited sample of historical radar data, few studies have explored the potential of using radar-derived precipitation estimates to construct extreme precipitation climatologies. In the United States, Frederick et al. (1977) used the (now outmoded) WSR-57 radar to develop area-depth curves. Area-depth curves have been traditionally used as a means of converting point (i.e. station) rainfall extremes to values representative of larger geographic areas, such as river basins. US Weather Bureau Technical Publication 29 provides a set of these areal reduction factor (ARF) curves (based on rain gauge data) for the contiguous US (USWB, 1957). Allen and DeGaetano (2005) review the TP-29 methodology and assess several of the assumptions used in this publication.

In Frederick et al.'s approach, radar reflectivity is subsequently converted to rainfall rate, R in mm h^{-1}, by the following Z–R relationship:

$$Z = 55R^{1.6}. \tag{1}$$

Using four 'large' storms (at least one grid point with ≥ 25 mm of precipitation in 1 h) near Norman, Oklahoma, prototype ARF curves were developed for watershed areas up to 1500 km^2 and accumulation periods ≤ 1 h. Substantial differences between Frederick's radar ARF curves and those given in TP-29 were noted. The 30-min radar ARF was considerably larger than that derived from the gauges over all basin sizes. Beyond an area of ~ 690 km^2, the slope of the TP-29 ARF curves approaches zero, while the radar ARFs continued to decay.

Similarly, Stewart (1989) exploited the high temporal (and spatial) resolution of radar data to develop hybrid raingauge-radar ARF relationships for Northwest England. Limited by the small amount of radar data available (98 days), the analysis focused on the relationship between short duration (≤ 12-h) and 24-h areal rainfalls. For each heavy rainfall event, the ratio of the maximum areal short duration rainfall to the corresponding daily areal rainfall total was calculated and ultimately an average ratio over all events obtained. Using these ratios, ARF-area curves based on daily rain gauge data were modified to sub-daily ARF-area curves.

Despite the uncertainties inherent to radar precipitation estimation, as radar and computational technology continues to evolve, radar data has the potential to become the preferred source of high-resolution rainfall data. Current US National Weather Service Weather Surveillance Doppler Radars (WSR-88D) provide nearly complete coverage of the contiguous United States at 10,000 feet (3.05 km) above site level (Klazura and Imy, 1993). It is unclear as to whether this data can be exploited to improve current estimates of extreme areal precipitation events. When based on in situ rain gauge observations, these precipitation extremes are fraught with uncertainties related to spatial interpolation based on a widely spaced observation network. Conceivably the use of radar data will eliminate the need for spatial interpolation. However, the veracity of the radar rainfall estimates, particularly in terms of extreme events, may compromise the use of these data in developing extreme areal rainfall climatologies.

In this study a set of prototype radar ARF curves are developed (since only 5 years of data are currently available) and compared with those obtained using a relatively high-density rain gauge network. Although it is questionable that the ARF methodology will be preferred once an adequate record of radar data exists, this approach offers a convenient means of comparing the radar and gauge data in the context of an established method of areal extreme rainfall estimation. Furthermore, it identifies several potential sources of discontinuity between existing gauge and future radar-based climatologies. Two geographic regions are evaluated to isolate the effect of moderate differences in topography. Our data and methodology, including a brief discussion of the techniques to calibrate the radar estimates using gauge data, are described in Section 2. In Section 3, several analyses are presented to explain the observed differences between the radar and gauge areal extremes.

These lead to several conclusions that are presented in the final section.

2. Data and methodology

2.1. Radar data

Although an understanding of the physical mechanisms by which radar is used to estimate rainfall is necessary to fully understand these problems, this paper is not the proper venue for such a review. Interested readers are referred to Doviak and Zrnic (1993) or Rinehart (1997) for more detail in this area.

Despite the advantages of enhanced spatial and temporal resolution, radar precipitation estimates are prone to inaccuracies, with errors often as large as 200% (Baeck and Smith, 1998). Multiple factors contribute to these errors. These include changes in the precipitation before it reaches the ground (e.g. evaporation), beam blockage by obstacles close to the radar site (e.g. ground clutter), as well as hardware calibration errors. Attenuation of the signal by the atmosphere and variations in the relationship between backscattered energy and rainfall rate also contribute to estimation errors.

Radar data for the 5-year period from 1996 to 2000 was acquired from the Global Hydrology Resource Center (GHRC) via the Internet at http://ghrc.nsstc.nasa.gov. The GHRC generates 2×2 km daily rainfall products for the continental United States based on 15-minute composites of reflectivity from WSR-88D network. The reflectivity data is converted to rainfall depth by setting $A=300$ and $b=1.4$ (Woodley et al., 1975).

The daily rainfall totals are based on a 24-hour accumulation from 00:00 UTC to 23:59 UTC and grouped into one of the 13 accumulation bins given in Table 1. For purposes of analysis, each bin was assigned a discrete accumulation equal to the midpoint of its assigned range (Table 1). Daily accumulations greater than 12.70 cm were set to 15.24 cm to provide a single value for this unbounded bin. Bin width increases with increasing daily accumulation, ranging from 0.254 to 2.54 cm. Although daily rainfall totals reported to the nearest millimeter would have been desirable, the use of discrete accumulation bins did not appear to adversely affect our analysis.

Table 1
The 13 levels of daily radar rainfall accumulation (cm) used by the GHRC and the corresponding discrete accumulation (cm) used for calculation of radar ARF

Level	GHRC Accumulation	Discrete accumulation
0	0	0
1	(0–0.254]	0.127
2	(0.254–0.508]	0.381
3	(0.508–1.016]	0.762
4	(1.016–1.524]	1.27
5	(1.524–2.032]	1.78
6	(2.032–2.54]	2.29
7	(2.54–3.81]	3.17
8	(3.81–5.08]	4.45
9	(5.08–7.62]	6.35
10	(7.62–10.16]	8.89
11	(10.16–12.70]	11.43
12	>12.70	15.24

2.2. Rain gauge data

Daily precipitation data from the NOAA Cooperative Observer Network (Coop) were used as a benchmark for comparison with the radar estimates. The distribution of rain gauges across the country is not uniform, with two notable areas of high station density located in northern New Jersey and southwest North Carolina (DelGreco, Personal Communication). Both regions possess at least 1 gauge per 32.2×32.2 km grid, with many of the grids having between 3 and 4 stations. These two locations also exhibit climatological and topographic differences allowing an assessment of these geographic differences on ARF.

In both New Jersey (NJ) (Fig. 1a) and North Carolina (NC) (Fig. 1b) the study area encompasses 18,000 km^2. In NJ, 22 Coop stations comprise a low-density rain gauge network ($gauge_{low}$). In addition, a high-density network ($gauge_{high}$) consisting of 38 Coop and 5 New Jersey Home Net stations (NJHN) was also evaluated. Daily precipitation data for the NJHN stations, along with metadata, were acquired from the Office of the New Jersey State Climatologist via the Internet at http://climate.rutgers.edu/stateclim/. Similar station densities were available in NC. The low-density network consists of 20 Coop stations, and the high-density network 33 Coop stations. The low-density networks are subsets of the high-density network, which subjectively maintain adequate spatial coverage of the basin. The use of two networks

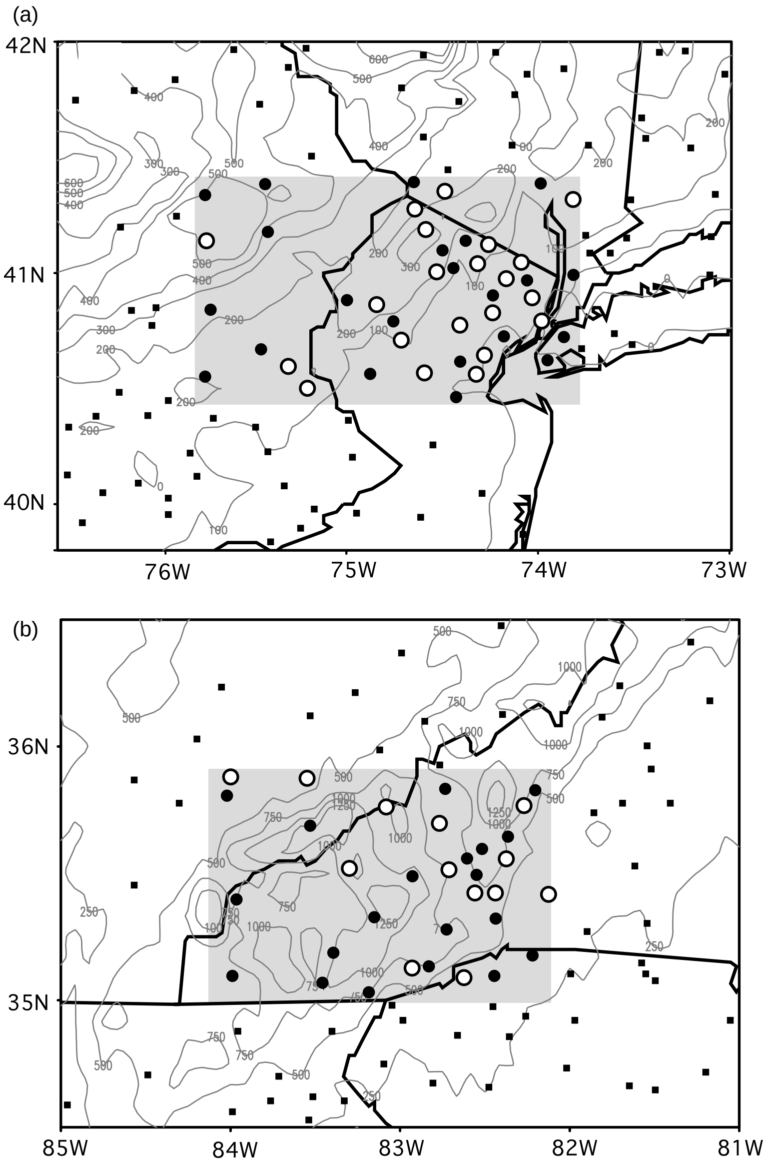

Fig. 1. Location of high (both open and closed circles) and low (closed circles) density network rain gauges in (a) New Jersey and (b) North Carolina. Gray elevation contours (meters), the location of rain gauges outside the study areas (black squares) and basin outlines are also included.

provided a means of evaluating the influence of station density on ARF. In both cases, additional stations outside the basin were used to interpolate mean areal precipitation within the basin (Fig. 1). Smaller sub-basins were constructed by systematically partitioning the 18,000 km^2 basin into sub basins that encompassed smaller areas.

2.3. Data processing

The radar precipitation estimates provided a third network of rainfall observations. Within each basin, a total of approximately 4500, 2×2 km radar pixels comprised this network. A time of observation adjustment procedure outlined by Allen and

DeGaetano (2005) was applied to all gauges so that the standard observation hour coincided with the 0000–2359 UTC accumulation period of the radar data. Analyses were conducted and showed that the subsequent results were resilient to differences in observation time.

The large size of an individual raw daily radar file, precluded the computation of an areal radar precipitation total on each day. Rather, the computation of these values was (1) limited to days on which the gauge network experienced one of the five largest annual areal average precipitation events, and (2) days on which any of the individual gauges reported one of its five largest annual precipitation events. Still, this resulted in the computation of about 50 areal precipitation totals per year.

2.4. Computation of ARF

Areal reduction factors (ARF) were used as a means of comparing the radar and gauge derived areal precipitation extremes. ARF essentially transforms point rainfall depths to an equivalent rainfall depth over an area, with the same probability of exceedence as that of the point rainfall. TP-29 (U.S. Weather Bureau, 1957) is perhaps the most common source of ARF for the US TP-29 defines ARF as:

$$\mathrm{ARF}_{TP-29} = \frac{\frac{1}{n}\sum_{j=1}^{n}\hat{R}_j}{\frac{1}{k}\sum_{i=1}^{k}\left(\frac{1}{n}\sum_{j=1}^{n}R_{ij}\right)} \quad (2)$$

where $\hat{R}_j$ is the annual maximum areal rainfall for year j, R_{ij} is the annual maximum point rainfall for year j at station i, k is the number of stations in the area, and n is the number of years. It is not a requirement that $\hat{R}_j$ and R_{ij} occur on the same date. Areal rainfall, of duration t, is simply an unweighted average of each station's t-duration point rainfall. In all cases ARF-area curves for the 1996–2000 period were calculated using Eq. (2). Given that Eq. (2) is based on the average of the five rainfall extremes, the ARF curves approximate events with a 2-year return period.

Differences between the spatial resolution of the radar and gauge networks and the precision of the rainfall values (discrete bin intervals versus 0.25 mm observation resolution) required the evaluation of several different procedures for calculating radar-based ARF. In the first method (radar$_{\mathrm{RG}}$) the radar pixels were used as surrogates for the individual gauges. Gauges were paired with the closest (in terms of distance) radar pixel and this limited set of radar data was used to compute ARF based on the density and location of the station networks (both high and low-density). As with the original gauge data, mean areal precipitation was calculated as an unweighted average of the limited subset of radar pixels to conform with the TP-29 methodology. Allen and DeGaetano (2005) show that this simple approach to computing areal precipitation results in ARF curves that deviate only minimally from curves using areal averages based on inverse distance weighting or Theissen interpolation.

The second method (radar$_{\mathrm{AP}}$) capitalized on the high spatial resolution of the radar estimates. Each of the 4500 pixels was treated as a separate rain gauge site. Again the computation of areal precipitation was based on an unweighted average of each of this large array of precipitation estimates.

Operationally, it is unclear how to best incorporate radar precipitation estimates into extreme areal precipitation climatologies. A number of different approaches are feasible, each with its own strengths and weaknesses. For instance, it is possible to use a long series of radar-based areal totals to directly compute the rainfall amounts associated with different return intervals. Although this is appealing in that it is the most direct use of the radar data, it necessitates the computation of unique areal rainfall extremes for each of an infinite number of basin areas and geometries. Such an approach would not be feasible for developing regional or national extreme areal rainfall climatologies. Conversely, a hybrid approach using the TP-29 methodology with radar data capitalizes on both the enhanced spatial resolution of the radar data and the transferability of the results to an array of basins. Since the combination of these two attributes is appealing, this work focuses specifically on the incorporation of the radar data into the TP-29 methodology. Nonetheless, the direct computation of areal precipitation amounts for different return intervals using the radar estimates is necessary for the evaluation of the TP-29 procedure. This allows a preliminary quantitative analysis of the areal extremes given by the two approaches, albeit using a limited set of observations.

2.5. Radar rainfall calibration techniques

Based on monthly and seasonal studies, areal precipitation estimates based on all available radar pixels are too small (∼50%) compared to the corresponding gauge derived areal precipitation (Schmidt et al., 2000; Stellman et al., 2001). Similarly, studies investigating hourly accumulations at individual radar sites have shown a proclivity for the radar to underestimate compared to the gauge (Smith et al., 1996; Beack and Smith, 1998). Comparatively few studies have examined the accuracy of radar derived extreme precipitation. Those that have, generally conclude that radar also tends to underestimate gauge-measured precipitation associated with these extreme events (Baeck and Smith, 1998; Vieux and Bedient, 1998; Lott and Sittel, 1996; Wilson and Brandes, 1979). The degree of underestimation is highly dependent on the storm, with the heaviest rainfall underestimated by more than 40% in some cases.

By itself, the influence of the underestimation of radar-estimated precipitation on ARF is unclear, as it influences both the numerator and denominator of the ratio. Thus, if the underestimation of the areal and point-specific totals is similar it is possible that only a minimal change in ARF will result. However, if the degree of underestimation for the areal total is smaller in comparison to that associated with a subset of specific points, ARF may be overestimated. Woodley et al. (1975) suggest such a pattern of disportionate bias. To quantity the effect of the radar biases, two calibration methods based on rain gauge observations were employed. Although adjusting the parameters in Eq. (1) is also a feasible approach for improving radar estimates of extreme precipitation, it is difficult to address the range of potential *Z–R* relationships, particularly since smaller scale variations in the relationship likely exist within individual storms.

Several authors (e.g. Wilson and Brandes, 1979; Fulton et al., 1998; Sauvageot, 1994; Chojnicki et al., 2000) have proposed methods for the calibration of radar data with rain gauge observations. It should be noted that rain gauges are known to be associated with their own undercatch bias due to wind-induced turbulence (Groisman and Legates, 1994). Nevertheless, throughout this study the gauge data is taken as the standard.

As multiplicative (Wilson and Brandes, 1979) and additive (e.g. Chojnicki et al., 2000) adjustments have been proposed, both of these approaches are evaluated.

For a given day and radar pixel, the three closest rain gauges with valid observations were identified. As the gauges were often a considerable distance from the base pixel, the three radar pixels closest to each gauge were also identified. Using these data, the adjusted radar rainfall accumulation at pixel k on day d, AR(k,d), was calculated by

$$AR(k,d) = R(k,d) \times \frac{1}{3}\sum_{i=1}^{3}\left[\frac{G(i,d)}{R(i,d)}\right] \tag{3}$$

where

R(k,d) = unadjusted radar rainfall at pixel k on day d,
G(i,d) = rainfall of the ith-closest gauge to pixel k on day d, and
R(i,d) = unadjusted radar rainfall at the pixel closest to the ith gauge on day d.

This multiplicative adjustment was applied to each pixel in the basin, yielding a set of gauge calibrated rainfall totals. This approach is similar to that used in NWS precipitation estimation algorithms, with two important exceptions. All gauge-radar pairs are weighted equally in the WSR-88D procedure as opposed to Eq. (3) that weights observations proportional to depth. In addition, the WSR-88D uses a single average bias adjustment, optimized through the use of a discrete Kalman filter, that is applied to all pixels. The additive bias adjustment followed a similar procedure based on the equation

$$AR(k,d) = R(k,d) + \frac{1}{3}\sum_{i=1}^{3}[G(i,d) - R(i,d)] \tag{4}$$

In both cases, radar pixels measuring no precipitation were excluded from adjustment.

The decision to use a spatially varying adjustment as opposed to a constant value, stems from previous studies. Smith et al. (1996) show a tendency for the Tulsa, Oklahoma WSR-88D to underestimate gauge rainfall at ranges less than 40 km due to the third and fourth elevation angles overshooting the precipitation. Rainfall was also underestimated at ranges greater than 150 km in the summer (>100 km in winter) due to lack of detection and incomplete beam filling of the larger volume of air. At intermediate ranges amplification of the rainfall statistics occurs, especially during the cold season due to the bright band effect. Similarly, Chojnicki et al. (2000) show that combining daily radar and gauge data using a spatially varying bias adjustment gives the most accurate daily rainfall estimates based on seven automated weather stations in Georgia.

3. Results

Fig. 2 shows radar and gauge ARF curves based on the low and high-density gauge networks. ARF-area points are fit using a nonlinear least squares fit to an exponential model. In all cases r^2 exceeds 87%. These radar precipitation estimates were not adjusted based on the rain gauge observations For both radar and gauge data, the difference in high and low density ARF is minimal. Similarly, the radar$_{AP}$ ARF corresponds well with the low and high-density radar$_{RG}$ ARF. Fig. 2a and b show that the effect of omitting Hurricane Floyd, in which numerous pixels were placed in the unbounded GHRC accumulation interval (Table 1). Although the ARF values including Floyd are higher, as expected, the clustering of the curves based on the gauge and radar data is evident in both cases. In all cases for a given platform, it appears the density of observations does not have a substantial effect on the ARF-area relationship, even with the very high density of the radar$_{AP}$ data. However, the most striking feature in Fig. 2a and b, is the considerable difference in radar ARF compared to gauge ARF. The radar ARF decays much quicker than the gauge ARF. At 20,000 km^2, the difference between radar ARF and gauge ARF is nearly 0.10.

These two general findings, little variation in ARF with the spatial density of observations and a more rapidly decaying radar ARF, also hold for the North Carolina study area (Fig. 2c). In this region, the difference between radar and gauge ARF is larger than in New Jersey. It should be noted, that the exponential fit to the ARF values is poor when all radar pixels are considered. In this case, r^2 falls below 40% primarily due to the spread of values associated with subbasin areas <1000 km^2. Eliminating the values for these small basins increases r^2 to 71%.

The locations of the smallest NC sub-basins were constrained to the area that maximized rain gauge density. As this area was confined to the northeast quadrant of the study area, these basins are a poor sampling of the entire study area. Radar$_{AP}$ ARF is relatively low for these five basins due to the topography and higher spatial variability of the radar's extreme precipitation (compared to gauges). Re-calculating the average radar$_{AP}$ ARF for 10 small basins located throughout the NC study area, improves the logarithmic regression as evidenced by a new r^2 of 83%. This apparent bias due to basin location is discussed more fully in a subsequent section.

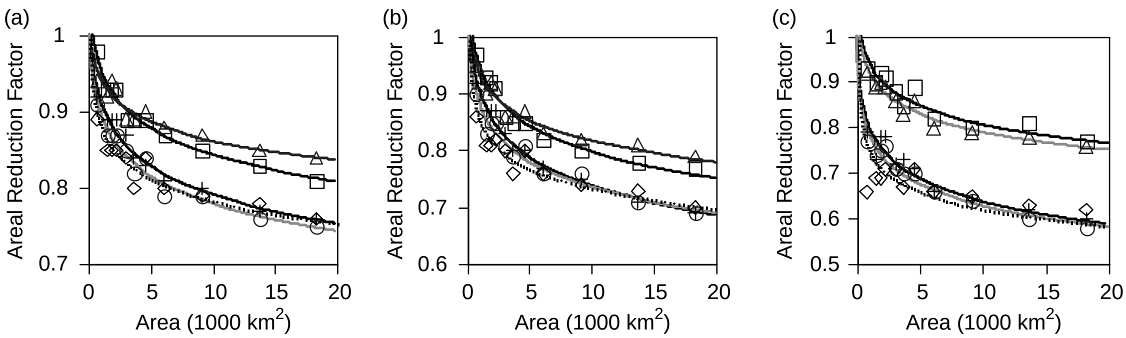

Fig. 2. ARF curves for (a) New Jersey; (b) New Jersey with Hurricane Floyd excluded; and (c) North Carolina. Curves correspond to the 2-year return interval based on the low (top black, squares) and high (top gray, triangles) density Coop network, the low (bottom black, crosses), high (bottom gray, circles) density radar$_{RG}$ networks and the radar$_{AP}$ network (bottom dotted, diamonds).

3.1. Coincidence of gauge and radar precipitation maxima

It is possible that the difference between radar and gauge ARF is due to a disparity in the dates on which annual maximum rainfall (both point and areal) occur when based on radar as opposed to the gauges. For all basins, simultaneous radar and gauge maxima occur in only one-third or less of the cases in both areas (excluding Hurricane Floyd in NJ). Thus, the gauge and radar ARF curves are based on different events with different magnitudes and spatial structures. Both of these attributes impact the ARF-area relationship. To quantify this difference, radar ARF was computed based on the radar-estimated precipitation amounts that occurred on those days that experienced maximum gauge and areal rainfall. This had a profound effect on the previous radar ARF relationship (Fig. 3). Except for the largest NJ basins, these hybrid ARF values exceed 1.0. This is a reflection of the poor correspondence between radar and gauge extreme precipitation occurrence. For ARF to exceed 1.0, the numerator of Eq. (2), representing the *n*-year average of annual maximum areal precipitation must exceed the n-year, and *k*-station average of annual maximum point rainfall amounts.

Using the NJ basin as an example, the average maximum areal precipitation is 8.74 cm when based on the 43 gauges, and only slightly higher (9.32 cm) when based on the radar data from the same days. However when the k-station average of annual maximums is large, that derived from radar (on the same days) is relatively small. Here, the values for the NJ basin are 10.45 cm from the gauges, but only 8.23 cm for the same-day radar estimates. This implies that the radar underestimates rainfall depths corresponding to the annual gauge maxima. On average, over the 5 years and 43 stations in the NJ basin, the underestimation is nearly 50%. In some cases, the underestimation exceeds a factor of 10 (9.68 vs. 0.381 cm at Bound Brook in 2000). This disparity, similar areal rainfall totals, but a large underestimation of point rainfall, drives the observed differences in the ARF curves.

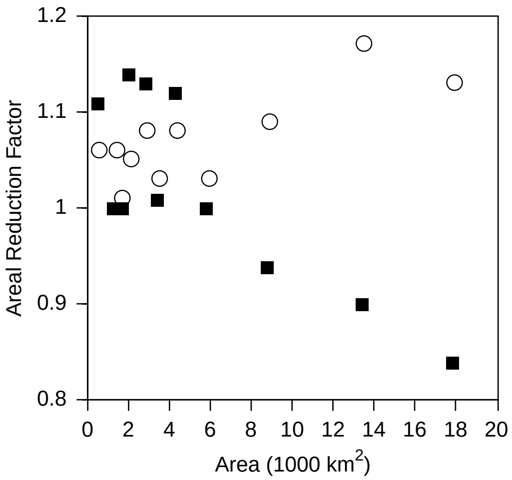

Fig. 3. ARF values based on the the high density radar$_{RG}$ network for the dates of the annual maximum point and areal events based on the NJ (squares) and NC (circles) gauges.

3.2. External influences

It is possible that differences in observation time were in part responsible for some of the differences between gauge and radar-based extreme station rainfall noted above, despite the use of the Allen and DeGaetano (2005) method to adjust the gauges to a 2000 local time observation schedule to approximate the 00:00 UTC to 23:59 UTC radar rainfall accumulation period. To address this concern, ARF-area curves for NJ and NC were calculated based on the subset of high-density networks' stations that maintained a morning (either 0700 or 0800 LT) observation schedule. This observation time maximized the number of available stations. Few stations reported an observation time corresponding to the radar accumulation interval. A comparison of the ARF curves developed using this network with those using the full suite of stations adjusted to the radar accumulation interval indicated that the observation time adjustment was not a major contributor to the difference between gauge and radar ARF.

It is also possible that the binned form of the radar data may have affected the comparison results. The binning procedure may have enhanced or reduced the data's variability. When neighboring pixels have precipitation totals that bracket a bin boundary, variability is increased as these two similar amounts are assigned values representing the midpoint of the neighboring bins. Alternatively, when adjacent pixels have precipitation amounts corresponding to the upper and lower limits of a bin, both of these values are assigned the same precipitation amount, reducing variability. Clearly, this effect is a function of bin width.

To quantify the effect of binning, the gauge data were binned to replicate the radar data (Table 1) and binned gauge ARF curves were constructed. Overall the differences between binned and non-binned gauge ARF was small, especially in the North Carolina study area.

3.3. Spatial precipitation variability

The between-station variability of extreme precipitation has important influences on ARF. Consider an ARF value for an individual year. This factor approaches 1.0 as the number of stations with coincident (same day) annual maximum precipitation increases.

As the between-station variability of precipitation increases, (particularly that within the largest events) the tendency to have many stations with coincident annual maximums decreases. Thus, the highest areal precipitation events are predominately composed of station precipitation totals that are less than each station's annual maximum precipitation accumulation. While an increase in between station precipitation variability has no effect on the denominator of Eq. (2), an increase in spatial variability acts to reduce the numerator, leading to lower values of ARF. Conceptually this could explain the lower values of radar ARF shown in Fig. 2.

An exception to this argument occurs in years when a highly variable, but uniformly extreme event occurs at the majority of stations. For example, in Hurricane Floyd, although the between station variance was relatively high ($\sigma^2 = 29.27\ \mathrm{cm}^2$), all stations received their annual maximum precipitation in this event. Thus the ARF during this single unusual year was 1.0, despite the high spatial variance.

In general, as the magnitude of an areal precipitation event increases, the corresponding between-station standard deviation, σ_{bs}, increases, especially for larger areas (Konrad, 2001). In the NJ basin, using data from 1949–1995, the correlation coefficient between annual maximum areal precipitation and σ_{bs} is 0.60 (0.49 in NC). Based on the 1996–2000 data, the corresponding correlation coefficients are higher (0.93 in NJ and 0.53 for NC). Given this dependence on storm magnitude, the coefficient of variation,

$$CV = \frac{\sigma}{\bar{x}} \times 100 \tag{5}$$

provides a more robust measure of rainfall variability, relative to the mean $\bar{x}$. It allows the variability of maximum areal precipitation to be compared between different extreme events (as well as different observation platforms). A small CV indicates a large mean areal precipitation event with small relative variability. In such cases ARF will tend to be high. Conversely, a high CV is associated with a less extreme mean areal precipitation event with large relative variability. Small ARF values are expected in such instances.

Fig. 4 compares CV based on gauge and radar$_{RG}$ data. Here, pairs of points do not necessarily represent the CV for the same event. Rather they represent CV of the specific radar- and gauge-derived annual maximum event (these can be different events for each platform) for a given year and basin. For NC (Fig. 4b), the majority of points fall above the 1:1 line, indicating a higher CV is associated with the radar estimates.

The corresponding plot for NJ is shown in Fig. 4a. Hurricane Floyd has been omitted since the radar binning procedure artificially reduces CV. The CV associated with the radar estimates is still larger than that for the gauge, but the dissimilarity is not as large as in NC. There is a substantial difference, however, between radar and gauge σ_{bs} in NJ. Averaged over all NJ sub-basins, the median (based on annual maximum events) gauge σ_{bs} is 1.65 cm whereas the median radar σ_{bs} is 3.30 cm. Disproportionate overestimation of observed precipitation by the radar in the NJ basin may act to reduce CV (via overstimation of x) in this region to a greater degree than in NC.

When CV is computed based on all radar pixels, rather than just those corresponding to a gauge, results similar to Fig. 4 are obtained in both regions. There is little difference in CV between the two densities of radar observations. Likewise when CV is computed based on radar data, but restricted to those days when areal average gauge precipitation is maximum, the results do not vary substantially from those in Fig. 4. Thus in all cases, the larger between-station (pixel)

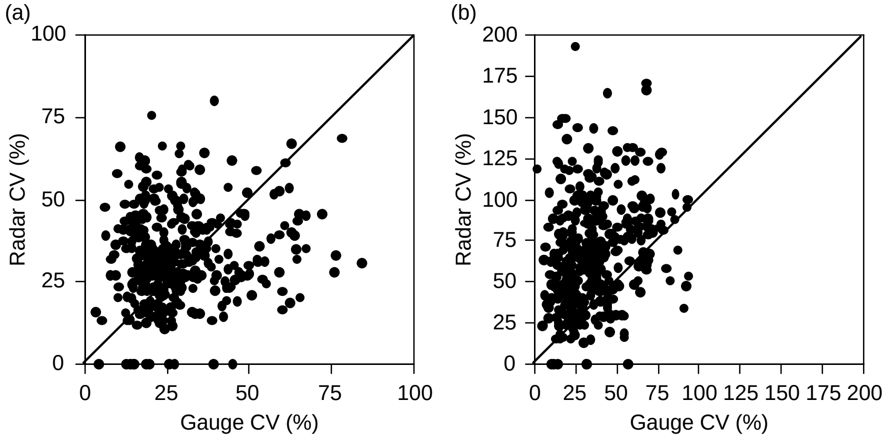

Fig. 4. Comparision of coefficient of variations (CV) associated with annual maximum areal precipitation based on the high density radar$_{RG}$ data and high density gauge network in (a) New Jersey (without Floyd) and (b) North Carolina. The 1:1 line is shown for reference.

variability associated with the radar data contributes to the lower ARF values in Fig. 2.

Related to the spatial variability of precipitation observations is the number of stations in a basin that have coincident (same day) annual maximum point precipitation events. In general, ARF will increase with the number of coincident annual maxima. To quantify this notion, the percentage of stations with annual maximums on the same day (for each year and basin) was calculated (based on both gauge and radar$_{RG}$ data) and the largest of these percentages identified. This value is denoted p_1. Table 2 shows that p_1 is highly correlated with ARF for both sensors, with correlations ranging from 0.61 to 0.85. These correlations are higher than those between CV and ARF, which although statistically significant were typically lower (-0.3 to as high as -0.88).

Fig. 5 shows that, on average, a higher percentage of gauges have coincident annual maximums than do the radar pixels that correspond to these gauges. In NJ, the median difference in p_1 (radar–gauge) is -16%, while this value is -14% in NC. This is also true when comparing p_1 based on the gauges with that using all radar pixels. This disparity between the gauges and radar also contributes to the lower radar ARF values in Fig. 2.

3.4. Seasonal biases

Table 3 shows the percentages of annual maximums that occur during the warm (April–September) and cold (October–March) seasons based on radar and gauge point and areal precipitation. In both regions, the radar annual maxima consist of more warm season events than those for the gauges. Including Hurricane Floyd, over 75% of the radar point and areal maximum events occur during the warm season in NJ. Based on the NJ gauge data, the maximum areal events are more evenly distributed between the two seasons, while more than two-thirds of the station maxima occur during the warm season. In NC, a similar number of annual areal maximum radar events

Table 2
Correlation coefficients of ARF versus p_1 based on radar and gauge data in both study areas. Correlations are based on each platform's annual maximum areal event in each basin

New Jersey			North Carolina		
Gauge$_{high}$	Radar$_{RG}$ (high density)	Radar$_{AP}$	Gauge$_{high}$	Radar$_{RG}$ (high density)	Radar$_{AP}$
0.71 (0.77)	0.64 (0.75)	0.74 (0.85)	0.73	0.61	0.81

Values in parenthesis show the effect of including Hurricane Floyd data.

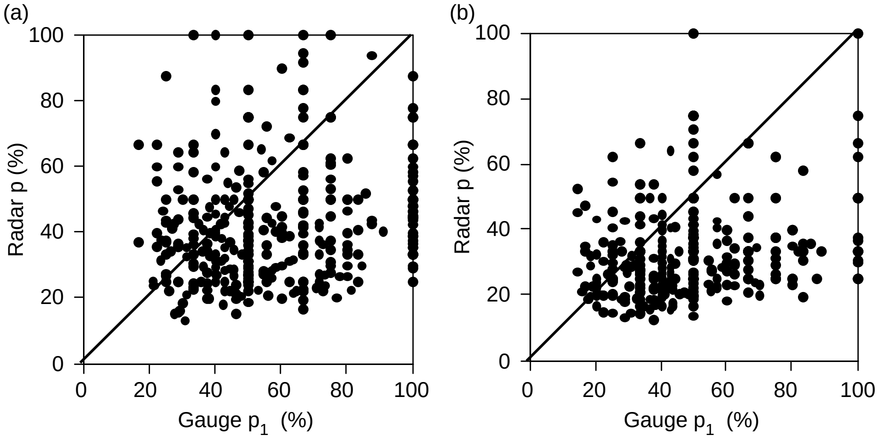

Fig. 5. As in Fig. 4, but for p_1.

occur during each season. This dichotomy between gauge and radar also extend to the point values, with more (less) cold season maxima noted for the gauges (radar).

These seasonal differences between radar and gauge data influence the resulting ARF curves. In both regions, warm season rainfall is generally convective and thus tends to exibit high spatial variability. Cool season events, however, are characterized by spatially uniform, synoptic-scale precipitation processes. This implies that ARF values based on a higher percentage of warm season events (as is the case with the radar data) will generally be lower. Conversely, when derived from mainly cold season events (as in the case of the gauges), ARF values tend to be higher. The seasonal difference between radar and gauge extreme precipitation favors a radar ARF that is less than that based on the gauges, as shown in Fig. 2. Rainfall from tropical systems is an exception, as illustrated by the decrease in ARF when Hurricane Floyd is omitted from Fig. 2.

If such seasonal biases are the primary contributor to the differences between the radar and gauge curves in Fig. 2, then calculating single-season ARF curves should reduce the difference between the curves. Such curves are shown in Fig. 6. Here, the r^2 for the exponential fit is at least 88%, except for the cold season gauge (60%) and radar (77%) ARF for NJ. As expected, smaller ARF values are indicated for the warm season events. During the warm season, the difference in ARF between the two instruments is essentially the same as that using annual data.

A comparable difference between gauge and radar ARF for cold season events is noted in NC. However, for NJ, the cold season ARF values from the two instruments are more similar. For a 20000 km^2 area the difference between the ARF values is only 0.04. Overall, as similar differences between radar and gauge-based ARF exist in both seasons, other factors must contribute to the disparities shown in Fig. 2.

Table 3
Percentage of annual maximums that occur during the warm and cold seasons based on radar and gauge data for the 1996–2000 study period

	New Jersey				North Carolina			
	Point		Areal		Point		Areal	
	Cold	Warm	Cold	Warm	Cold	Warm	Cold	Warm
$Radar_{RG}$	24 (20)	76 (80)	32 (25)	68 (75)	38	62	45	55
$Gauge_{high}$	44 (31)	56 (69)	62(44)	38 (56)	56	44	73	27

The percentages are shown for points (43 in NJ; 33 in NC) and basins (74 in NJ; 76 in NC). The NJ percentages with Hurricane Floyd are listed in parenthesis.

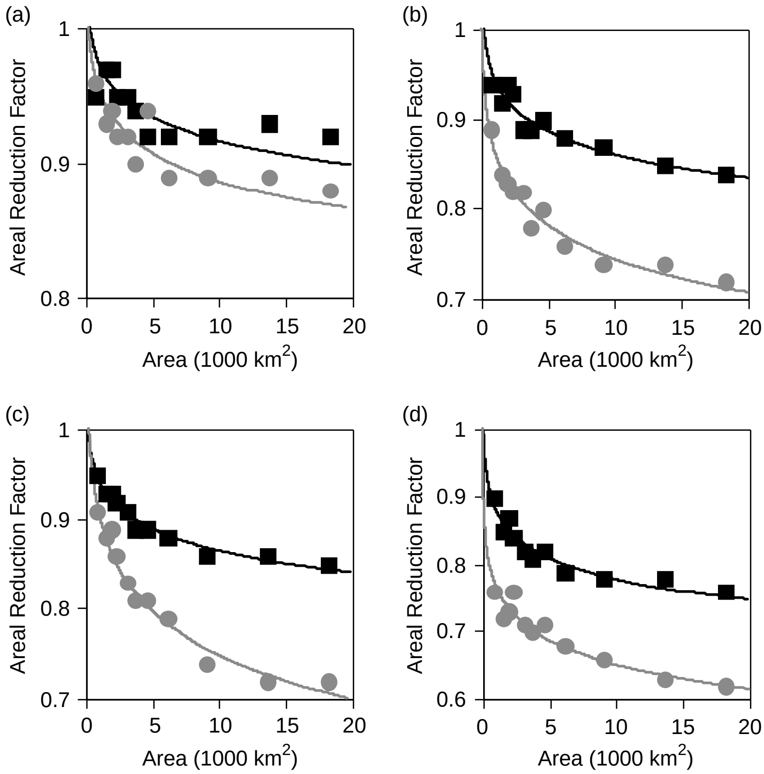

Fig. 6. ARF curves for the New Jersey study area stratified by (a) cold season and (b) warm season events and for the North Carolina study area stratified by (c) cold season and (d) warm season events. Values based on the $\text{gauge}_{\text{high}}$ network are given by the black line and squares. Those using the radar_{RG} network appear as gray lines and circles.

3.5. Gauge adjusted ARF curves

Table 4 shows median (over j years) values of the ratio R_i/G_i, where R_i is the radar's annual unadjusted maximum point or areal precipitation and G_i is the corresponding (same date) gauge precipitation, as in Eq. (3), but stratified by season. Here each annual ratio represents an average over all pixels in a basin and all basins in the study area. The median ratio is consistently larger for warm season events (both areal and point) than cold season events indicating that the radar tends to overestimate warm season events more than cold season events relative to the gauges.

The NJ radar data consistently overestimates the gauge values. Here the point data tend to be overestimated more than areal averages, particularly when Hurricane Floyd is included. In NC, annual point maximums are overestimated relative to the gauge, while areal precipitation is underestimated. Despite numerous previous studies that show a tendency for radar to underestimate precipitation (e.g. Stellman et al., 2001; Baeck and Smith, 1998; Lott and Sittel, 1996), it is not surprising that an overestimate is indicated. Here, the highest radar

Table 4
Median R/G biases comparing radar point and areal precipitation with the corresponding (same date) gauge point and areal precipitation

	Point			Areal		
	Annual	Cold	Warm	Annual	Cold	Warm
NJ	3.05 (2.94)	2.17 (2.35)	3.37 (3.02)	2.69 (1.79)	1.76 (1.71)	3.11 (2.58)
NC	1.33	0.88	2.10	0.83	0.68	1.32

Biases are shown for both study areas and stratified by annual maxima, as well as those annual maxima that occur during the cold and warm seasons. The NJ biases with Floyd are included in parenthesis.

totals are isolated *a priori* and compared to the gauges. Thus, those individual events in which radar precipitation is maximum (and presumably greater than the corresponding gauge value) are selected for use in the radar ARF calculation. Since ARF is defined as the ratio of average areal to average point precipitation, the radar's larger overestimation (compared to the gauges) of annual maximum point events compared to areal events could contribute to the lower radar ARF values indicated in Fig. 2.

This general overestimation of radar extreme precipitation estimates is also marked by considerable spatial variability (Fig. 7). These maps were compiled by taking the median ratio of the highest five annual radar events (1996–2000) to the corresponding precipitation at the gauge. In NJ (Fig. 7a), the radar

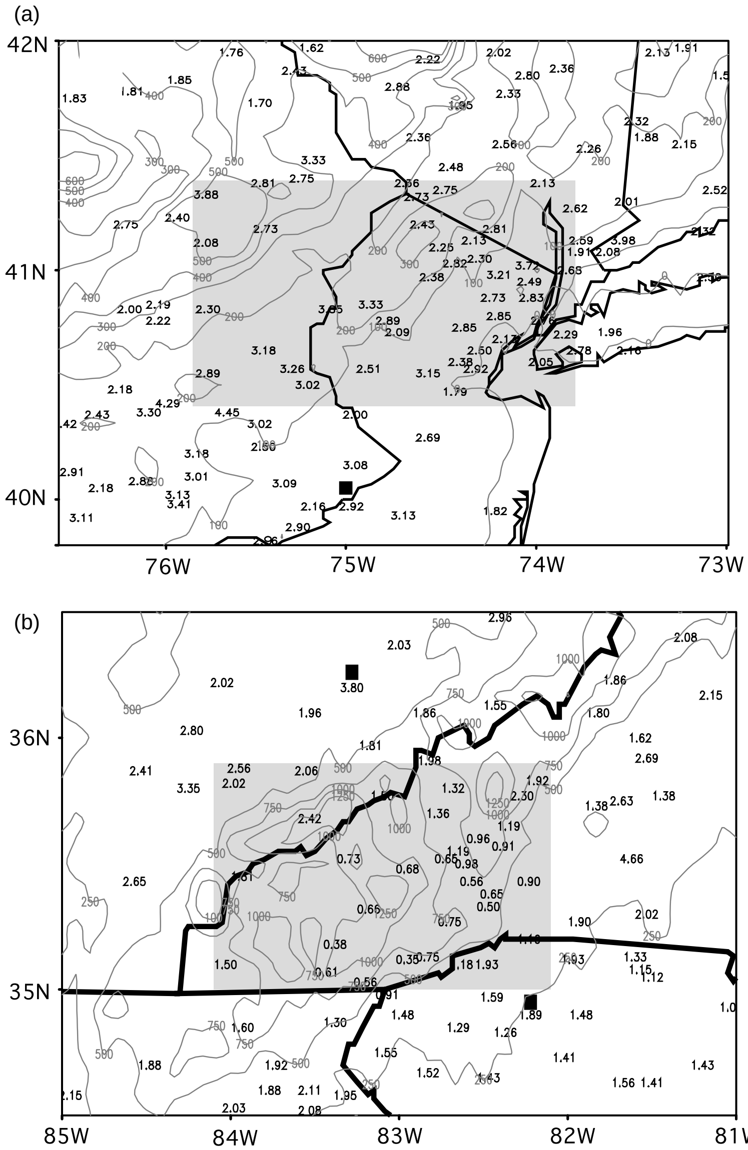

Fig. 7. Median R/G ratios based on the top five radar annual events (1996–2000) for each station in the (a) New Jersey and (b) North Carolina study area. Gray elevation contours (meters), the location of the WSR-88Ds (black squares) and basin outlines are also included.

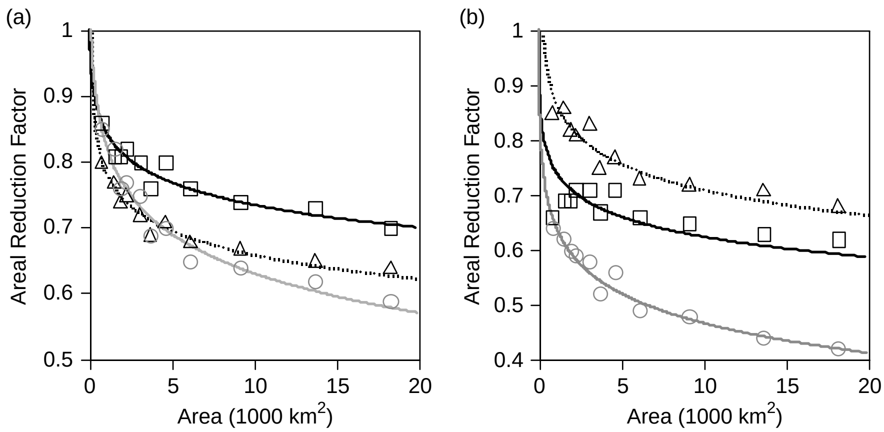

Fig. 8. ARF curves for the radar$_{AP}$ network (black, squares) and gauge calibrated radar$_{AP}$ data based on ratios (gray, circles) and differences (black dashed, triangles) for the (a) New Jersey (without Floyd) and (b) North Carolina study area.

tends to overestimate the gauge precipitation at all stations, in some cases by over a factor of 4. In the non-mountainous areas of North Carolina, the median point ratio is greater than 1.0, indicating overestimation. This is especially true in Tennessee, where the ratio exceeds 2.0. Despite the median ratio exceeding 1.0 for a few stations in the northeastern part of the basin, the radar tends to be biased towards underestimation in this more mountainous area. Across the entire NC basin the ratio ranges from 0.35 to 2.56 (Fig. 7b). The ratio is as high as 3.76 at a station outside the basin boundary.

An evaluation of the causes of the large radar biases that occur with extreme rainfall events is beyond the intended scope of this paper. Rather, we wish to explore the contribution of these biases to the differences between radar and gauge derived ARF.

The radar ARF curves from Fig. 2 were recomputed based on multiplicative and additive bias adjustments (i.e. Eqs. (3) and (4)).

A priori it was assumed that the calibrated radar ARF curve would lie between that of the unadjusted radar and gauges. This was generally not the case, with three of the four gauge-calibrated radar ARF curves falling below the corresponding unadjusted radar ARF curves (Fig. 8). For the multiplicative adjustment, the calibrated ARF values are smaller than those based on the uncalibrated radar estimates in both study areas. For NC basins larger than 5000 km^2, the calibrated values are 20% smaller.

These differences are influenced by changes in the spatial variability of the calibrated annual maximum point and areal radar rainfall amounts as different events comprise the set of annual maxima when the calibration is applied. Table 5 lists the average difference (adjusted-unadjusted radar) over all basin-years of the coefficient of variation ($\overline{\Delta CV}$), between-pixel standard deviation ($\overline{\Delta\sigma_{bs}}$) and the largest percentage of pixels with coincident annual maxima (p_1). These parameters were used previously to compare the gauge and unadjusted radar data.

In NC, the effect of the multiplicative adjustment is to increase both CV and s_{bs}, relative to the unadjusted radar data. Similarly, p_1 decreases slightly. Taken together, the changes in these parameters indicate a further increase in the spatial variability of the radar rainfall estimates following calibration. A similar increase in spatial variability (except for p_1 using the multiplicative adjustment and s_{bs} using the additive

Table 5
Average differences (adjusted–unadjusted radar) of p_1, CV and s_{bs} over all basin-years for New Jersey (without Floyd) and North Carolina

	New Jersey		North Carolina	
	G/R	*G−R*	*G/R*	*G−R*
p_1 (%)	8	−3	−3	11
$\overline{\Delta CV}$ (%)	16	5	26	−25
s_{bs} (cm)	0.69	−0.13	5.73	−0.34

Differences are shown for both the multiplicative (G/R) and additive (G-R) adjustment.

Table 6
The average bias adjustment ($\bar{x}$) and the corresponding average standard deviation ($\bar{\sigma}$) for extreme areal and point precipitation in New Jersey and North Carolina

	New Jersey		North Carolina	
	Point	Areal	Point	Areal
$\bar{x}$	1.71	1.23	5.65	3.96
$\bar{\sigma}$	1.63	0.52	4.8	2.06
$\bar{\alpha}$	0.4	0.53	0.69	0.97
$\bar{\omega}$	9.1	2.29	26.4	8.3

The average smallest ($\bar{\alpha}$) and largest ($\bar{\omega}$) adjustment at an individual radar pixel for each basin-year is also shown.

adjustment) is associated with calibration in NJ (both with and without Hurricane Floyd) (Table 5). Applying the additive adjustment to the NC radar data, however, produces higher ARF values, since this adjustment reduces the spatial variability of the estimates as indicated by an increase in p1 and a decrease in CV. Subsequent analyses focus on the multiplicative adjustment.

The average (over basin-years) bias adjustment and the corresponding average standard deviation (also over basin-years) of the adjustment for both same-day extreme areal precipitation and point annual maxima are shown in Table 6. As opposed to Table 4, these days are selected after calibration. On average, all adjustments increase the radar estimate, implying underestimation by the radar relative to the gauges. This, although in line with the literature (e.g. Stellman et al., 2001; Baeck and Smith, 1998; Lott and Sittel, 1996), apparently contradicts the earlier results (Fig. 7 and Table 4) which show overestimation by the radar, particularly in NJ. This is an artifact of which days comprise the annual extremes when the calibrated as opposed to uncalibrated radar estimates are used. In both regions, approximately 60% of the annual areal maximum calibrated events occur on a different day than those obtained using the unadjusted areal precipitation extremes. Furthermore, the occurrence of adjusted radar maximum rain events is skewed toward the cold season. This is a reflection of a higher proportion of gauge-based areal rain events during the cold season as compared to the unadjusted radar-based areal events (Table 3).

The second feature of Table 6 is that the average bias adjustments are large in magnitude (relative to typical 'extreme' rainfall depths in NJ and NC) and also exhibit large deviations. For example in NC, the average annual maximum areal precipitation adjustment is 3.96, with a corresponding $\bar{\sigma}=2.06$, while for station values, the adjustment averages 5.65 with a $\bar{\sigma}=4.8$. Thus, numerous radar pixels with low precipitation (relative to the gauge) receive very large adjustments, and as a result commensurate increases in estimated rainfall depth. These values are preferentially selected in the calculation of ARF (as opposed to more modest precipitation estimates that do not require substantial calibration). Despite the use of three neighboring gauges to minimize these large adjustments, such adjustments are still problematic given the high average adjustments and the excessive average maximum adjustment of 26.4 for a single pixel in NC. Apparently, the use of radar reflectivity to estimate station precipitation in the most extreme events is particularly challenging. The development of calibration techniques specific to extreme events is a prerequisite for the use of radar estimates in developing extreme rainfall climatologies.

4. Concluding comments

Clearly, extreme precipitation area-depth relationships exhibit differences when based on rain gauge versus radar precipitation data. Based on the proceeding analyses it can be concluded that:

1. Although both radar- and gauge-based ARF decline exponentially with increasing basin area, a much sharper decline is apparent for the radar data. Typically radar ARF values are 10–20% lower than those based on the gauge data.
2. Differences in which specific storms (the seasons in which they occur) constitute the most extreme precipitation events are one of the dominate factors responsible for the differences between gauge and radar-based ARF.
3. Along with different events, a disparity between the spatial variability of radar and gauge data also drives the observed differences in the ARF values. It is unclear which platform gives a more accurate measure of spatial variability.
4. Station density seems to have little influence on the depth-area relationships regardless of observation platform.

5. Although extreme rainfall amounts are considerably different between the radar and gauge networks, these differences in precipitation quantity do not in themselves drive the differences in the depth-area relationship.
6. Although there is general agreement between the results obtained from the NJ and NC networks, features such as storm characteristics, topography, radar proximity and in situ rain gauge location contribute to the more subtle differences noted between the regions. This suggests that the results could be extended beyond the eastern United States, provided a means of adjusting the WSR-88D precipitation estimates based on rain gauge data is available. The incorporation of technical advances such as polarization measurements into radar precipitation estimation algorithms also hold promise for the more widespread use of radar information in specifying areal precipitation extremes.

Having identified these differences, the question of which of these depth-area relationships is more accurate remains. If the radar data give a more accurate portrayal of the spatial structure (and hence areal rainfall accumulation) that a basin receives from extreme events, then current design considerations may be characterized as overly conservative. A definitive answer is beyond the scope of this paper, and will continue to be elusive until an adequate historical record of radar-based rainfall extremes becomes available.

Nonetheless as a means of stimulating further research in this area of applied climatology, 2-, 5-, and 10-year return period areal precipitation amounts were computed directly (as opposed to using ARF) using data for the period 1996–2000. This provided a means of comparing the actual precipitation extremes as opposed to the reduction factors. Table 7 compares radar- and gauge-based areal precipitation extremes computed directly (i.e. the beta-P distribution is fit to the time series of areal maxima that form the numerator of Eq. (2)). Return period amounts using the ARF relationships given by Allen and DeGaetano (2005) in conjunction with the 1996–2000 $\text{gauge}_{\text{high}}$ point precipitation amounts are also included for comparison. As the Allen and DeGaetano ARF curves are based on data from an earlier period (1949–1995), using this limited data record provides an independent data sample for comparing the two methodologies, albeit the station sample is not independent between the periods.

Table 7
Comparison of the 1996–2000 areal extreme precipitation (cm) calculated based on the direct fit of a beta-P distribution to the annual maximum areally interpolated gauge and radar data

	Return period		
	2-year	5-year	10-year
NJ			
Radar_{RG} (high density)	9.9	12.0	13.8
Radar_{RG} (low density)	9.4	12.0	14.4
Radar_{AP}	10.2	11.9	13.4
Calibrated radar_{AP}	6.5	11.4	17.4
$\text{Gauge}_{\text{high}}$	7.1	10.8	14.8
$\text{Gauge}_{\text{low}}$	7.0	10.6	14.6
Gauge ARF	7.2	9.5	11.8
NC			
Radar_{RG} (high density)	4.2	4.5	4.6
Radar_{RG} (low density)	4.1	4.4	4.6
Radar_{AP}	5.1	5.3	5.4
Calibrated radar_{AP}	6.6	8.3	9.8
$\text{Gauge}_{\text{high}}$	6.1	6.9	7.7
$\text{Gauge}_{\text{low}}$	6.4	7.5	8.5
Gauge ARF	6.0	6.8	7.5

Results are shown for a 18,000 km^2 basin in each study area. Return period amounts based on the ARF relationship given in Allen and DeGaetano are also given.

In both regions, the precipitation extremes cluster into groups representing the two observations platforms. As with ARF, the spatial density of observations has negligible effect on the areal extremes. In NJ and NC, the uncalibrated radar-based extremes are within 1 cm of each other. Likewise, the gauge networks yield comparable rainfall extremes between themselves and also the ARF-based value. For the 2-year and 5-year return intervals, the NJ radar extremes are consistently larger than those based on the gauges. This supports the finding that radar overestimated the maxima in NJ relative to the gauge. For the 10-year return interval, however, the bias is reversed, owing to the artificial underestimation of rainfall from Floyd due to the binning procedure. In NC, the gauge extremes are consistently 2–3 cm higher than those based on the radar, reflecting the tendency for the radar to underestimate precipitation extremes in this area.

Unlike the ARF relationships based on the calibrated radar data (Fig. 8), the direct fits of the extremes based on calibrated radar data are similar to those based on the gauge data. Overall, however, the magnitude and variability of the gauge adjustments are relatively large and hence, the accuracy of the adjustments for extreme events is questionable. Due to the poor correspondence between radar and gauge extreme precipitation, the utility of the radar data in providing direct estimates of extreme areal precipitation is uncertain.

Acknowledgements

This work was supported by NOAA grant NA17RJ1222. It represents a portion of the principal author's M.S. thesis, and thus thanks are extended to Drs Dan Wilks and Bill Philpot for their guidance, time and suggestions as graduate committee members. We are grateful to Dr. David Robinson, New Jersey State Climatologist, for supplying the NJ HomeNet data.

References

Allen, R.J., DeGaetano, A.T., 2005. Areal reduction factors for two e astern U.S. regions with high rain gauge density. J. Hydrologic Eng. In Press.

Baeck, M.L., Smith, J.A., 1998. Rainfall estimation by the WSR-88D for heavy rainfall events. Wea. Forecasting 13, 416–436.

Chojnicki, B., Hoogenboom, G., Georgiev, G.A., 2000. Estimation of rainfall intensity and spatial distribution based on data collected by automated weather stations and radar systems, Preprints, Twelfth Conference On Applied Climatology. Amer. Metor. Soc., Asheville, NC pp. 300–303.

Doviak, R.J., Zrnic, D.S., 1993. Doppler radar and weather observations. Academic, San Diego p. 562.

Frederick, R.H., Myers, V.A., Auciello, E.P., 1977. Storm depth-area relations from digitized radar returns. Water. Resour. Res. 13, 675–679.

Fulton, R.A., Breidenbach, J.P., Seo, D.J., Miller, D.A., 1998. The WSR-88D rainfall algorithm. Weath. Forecast. 13, 377–395.

Groisman, P.Y., Legates, D.R., 1994. The accuracy of United States precipitation data. Bull. Am. Meteorol. Soc. 75, 215–227.

Klazura, G.E., Imy, D.A., 1993. A description of the initial set of analysis products available from the NEXRAD WSR-88D system. Bull. Am. Meteorol. Soc. 74, 1293–1311.

Konrad, C.E., 2001. The most extreme precipitation events over the eastern United States from 1950 to 1996: considerations of scale. J. Hydrometeorol. 3, 309–325.

N. Lott, M. Sittel, 1996: A comparison of NEXRAD rainfall estimates with recorded amounts. Technical Report 96–03, National Climatic Data Center (NCDC), Research Customer Service Group, 28 pp.

Rinehart, R.E., 1997. Radar for meteorologists. Rinehart Publications, Grand Forks, ND p. 428.

Sauvageot, H., 1994. Rainfall measurement by radar: a review. Atmos. Res. 35, 27–54.

Schmidt, J., Lawrence, B., Olsen, B., 2000. A comparison of operational precipitation processing methodologies. Arkansas-Red Basin River Forecast Center p. 5.

Smith, J.A., Seo, D.J., Baeck, M.L., Hudlow, M.D., 1996. An intercomparison study of NEXRAD precipitation estimates. Water Resour. Res. 32, 2035–2046.

Stellman, K.M., Fuelberg, H.E., Garza, R., Mullusky, M., 2001. An examination of radar and rain gauge-derived mean areal precipitation over Georgia watersheds. Weath. Forecast. 16, 133–144.

Stewart, E.J., 1989. Areal reduction factors for design storm construction: joint use of raingauge and radar data, vol. 181. IAHS Publ. pp. 31–49.

U.S. Weather Bureau, 1957.Anon., 1957. Rainfall intensity-frequency regime—pt. 1, The Ohio Valley, TP-29. Dept. of Commerce, Washington, DC.

Vieux, B.E., Bedient, P.B., 1998. Estimation of rainfall for flood prediction from WSR-88D reflectivity: a case study, 17–18 October 1994. Weath. Forecast. 13, 407–415.

Wilson, J.W., Brandes, E.A., 1979. Radar measurement of rainfall: a summary. Bull. Am. Meteorol. Soc. 60, 1048–1058.

Woodley, W.L., Olsen, A.R., Herndon, A., Wiggert, V., 1975. Comparison of gage and radar methods of convective rain measurement. J. Appl. Meteorol. 14, 909–928.